RSC Advances

ROYAL SOCIETY OF CHEMISTRY

www.rsc.org/advances

RSC Advances RSCPublishing

ARTICLE

Polyimide nanocomposites with functionalized SiO_2 nanoparticles: Enhanced processability, thermal and mechanical properties†

Cite this: DOI: 10.1039/x0xx00000x

Received 00th January 2012,
Accepted 00th January 2012

DOI: 10.1039/x0xx00000x

www.rsc.org/

Young-Jae Kim,[a] Jong-Heon Kim,[b] Shin-Woo Ha,[a,c] Dongil Kwon,[*b] Jin-Kyu Lee[*a]

SiO_2-polyimide nanocomposites were successfully fabricated by surface modification of silica nanoparticles. In order to create structural similarity between the polymer and the SiO_2 surface and to generate interfacial interaction with the polymer chain, (3-trimethoxysilylpropyl) diethylenetriamine was attached to the surface, and then, the surface amines were reacted with phthalic anhydride. The modified silica nanoparticles in polyamic acid solution were subjected to thermal imidization to obtain SiO_2-polyimide (PI) nanocomposite films. Cross-sectional transmission electron microscopy results showed no significant aggregation in any of the SiO_2-PI nanocomposite films having up to 20 wt% of silica nanoparticles. The effects of silica nanoparticles as a filler material on the thermal, optical, and mechanical properties of the SiO_2-PI nanocomposite films were studied in comparison with those of PI by UV-Vis spectrometery, thermal gravimetric analysis, thermal mechanical analysis, and nanoindentation

Introduction

Polymer-inorganic nanocomposites have been studied extensively because inorganic nanomaterials can provide desirable properties such as high refractive index,[1] dielectric constant,[2] electrical conductivity,[3] thermal conductivity,[3] and hardness[4] to polymers when used as complementary additive components. Various inorganic nanomaterials such as clay, semiconducting nanocrystals, metal nanoparticles, and ceramic nanoparticles have been employed for those purposes.

In situ and ex situ synthesis are the primary methods used to prepare polymer-inorganic nanocomposites.[1] In situ synthesis methods generate nanoparticles inside a polymer matrix by in situ sol-gel reactions[5] or in situ gas-solid reactions[6], and therefore, one-step fabrication is possible. However, it is difficult to ensure full control of the shape, crystallinity, size, size distribution, and surface properties of the nanoparticles during the reaction. Moreover, the properties of the nanocomposites can be influenced by unreacted reactants or byproducts, which is usually considered to be a main drawback of in situ methods.[1] On the other hand, in ex situ synthesis methods, pre-made nanoparticles are blended with polymers, or the polymers are synthesized with the nanoparticles.[7, 8] Therefore, the properties of the nanoparticles can be easily controlled. Among ex situ synthesis methods, blending is the simplest and most convenient way to prepare polymer nanocomposites.[4] However, the nanoparticles tend to aggregate in large agglomers during the mixing process due to their high surface energy and low compatibility with polymers, which leads to deterioration of the mechanical and optical properties of the resulting composites. Thus, the key challenge with these methods are improving the compatibility of the nanoparticles with the polymer and maintaining good dispersibility within the polymer matrix. Modification of nanoparticle surfaces by chemical and/or physical interactions is generally employed to solve these problems.[4]

Aromatic polyimides are important industrial polymers used in many applications such as packaging and insulation for large-scale integrated circuits because of their high thermal stability, high chemical resistance, mechanical properties, and low dielectric constants.[9, 10] However, their disadvantages include high glass transition temperatures (T_g)[11, 12] and high thermal expansion coefficients (CTE).[9] The high T_g of polyimides, which is caused by their rigid back bones and strong interaction, makes them difficult to process.[11] In addition, the higher CTE of polyimides compared with that of metals causes interfacial stress induced by the thermal expansion mismatch between the polyimide and the metal during thermal cycling in the manufacturing process. This leads to device failure via interfacial decohesion or cracks in microelectronic applications.[13, 14] Many efforts to reduce polymer CTE have been undertaken by using inorganic fillers such as

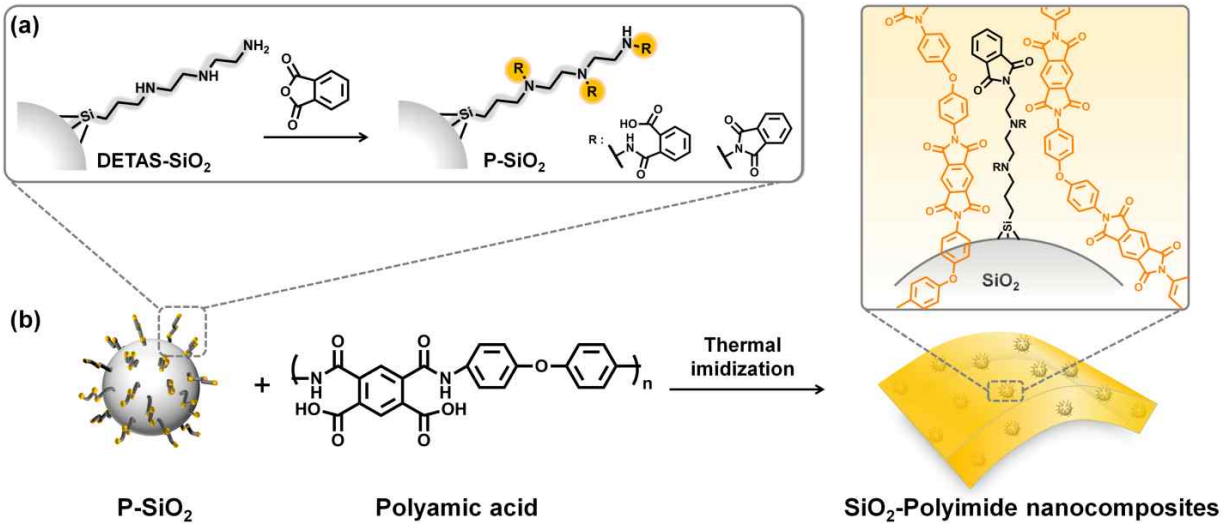

Fig. 1 Schematic illustrations of (a) the surface modification of silica nanoparticles by (3-trimethoxysilylpropyl) diethylenetriamine (DETAS) and the reaction between the suface amines and phthalic anhydride and (b) the fabrication of SiO_2-PI nanocomposite film by thermal imidization.

nanoparticles,[15] nanotubes,[16] and clay.[17] SiO_2 nanoparticles are most widely used as a nanofillers due to their low CTE (~0.55 $\times 10^{-6}$ $°C^{-1}$), high thermal stability, optical transparency, and easy surface modification.[18] There have been many attempts to fabricate SiO_2-polyimide nanocomposites in order to reduce the CTE of the polyimide. Most of the SiO_2-polyimide nanocomposites were prepared by the in situ sol-gel method[5, 9, 19-21] using a silica precursor, while only a few of them were prepared by blending processes.[15, 22, 23] Because polyimides and SiO_2 are incompatible, SiO_2 tends to accumulate in large aggregations in a polymer matrix.[22] To improve the compatibility between polyimide and SiO_2, surface modification of silica nanoparticles with oleic acid has been performed.[15, 23] However, no significant changes in thermal properties such as T_g and thermal decomposition temperature (T_d) were observed. Therefore, to obtain the desired properties of polyimide nanocomposites without aggregation of silica nanoparticles, an appropriate surface ligand to be used for the modification of the nanoparticles is needed.

Herein, we focused on the fabrication of SiO_2-polyimide nanocomposites by surface modification of SiO_2, using functional groups with chemical and structural similarities to the polymer chains. Silica nanoparticles prepared by the Stöber method[24] were modified by a simple two-step reaction: surface Si-OH groups were reacted with (3-trimethoxy-silylpropyl) diethylenetriamine (DETAS) to introduce a large number of amine sites onto the surface,[25] which could then react with phthalic anhydride, generating amic acid terminal groups (Fig. 1). We successfully incorporated silica nanoparticles up to 20 wt% in the polymers without aggregation, and compared the thermal, optical, and mechanical properties, along with the CTE, with those of the pristine polyimide to understand the effects of the silica nanoparticles.

Experimental

Materials

N-Methyl-2-pyrrolidone (NMP, 99%), poly(pyromellitic dianhydride-co-4,4′-oxydianiline) amic acid solution (12.8±0.5wt% in 80% NMP and 20% aromatic hydrocarbon), triethylamine (99%), phthalic anhydride (99%), and KBr (99%) were purchased from Aldrich. Ethanol (99.9%) was purchased from J. T. Baker, tetraethyl orthosilicate (TEOS, 96%) from TCI, and (3-trimethoxysilylpropyl)diethylenetriamine (DETAS, 95%) from Gelest. All organic solvents were used without any further purification.

Synthesis and modification of silica nanoparticles

2.5 mL of aqueous ammonium hydroxide solution and 2.5 mL of deionized water were mixed with 118 mL of EtOH. Then, 2.0 mL of TEOS was added and stirred for 12 h at room temperature. The silica suspension was centrifuged for 20 min at 20000 rpm. The precipitate was redispersed in EtOH, followed by centrifugation under the same conditions. This centrifugation-redispersion procedure was repeated more than two times. Further, the silica suspension was centrifuged at 3800 rpm for 10 min in order to remove any aggregated products, and the supernatant was collected for the next reaction.

4.0 mL of DETAS was added to the dispersed SiO_2 solution (400 mg of SiO_2 nanoparticles in 40 mL of EtOH), and the mixed solution was stirred at room temperature for 12 h. The mixture was centrifuged for 20 min at 20000 rpm, and then, the precipitate was redispered in EtOH. This centrifugation-redispersion procedure was repeated more than two times to obtain the dispersed solution of the DETAS-modified SiO_2 nanoparticles (DETAS-SiO_2). To the dispersed solution of

DETAS-SiO_2 in 40 mL of EtOH, 1.7 g of phthalic anhydride and 0.16 mL of triethylamine were added. The mixture was refluxed with vigorous stirring for 12 h. After cooling, the dispersion was centrifuged for 20 min at 20000 rpm, and then, the precipitate was redispered in *N*-methyl-2-pyrrolidone (NMP). This precedure was repeated more than two times to remove the excess phthalic anhydride and triethylamine. The dispersed solution was centrifuged at 3800 rpm for 10 min to remove any aggregated particles, and the dispersed solution of phthalic anhydride-modified silica nanoparticles (P-SiO_2) was reserved for the next process.

Preparation of SiO_2-polyimide nanocomposites

P-SiO_2 suspension (30 mg/mL in NMP) was added to appropriate amounts of poly(pyromellitic dianhydride-co-4,4′-oxydianiline) amic acid (PAA) solution to prepare the composite films containing 5, 10, 20, and 40 wt% of SiO_2. And then NMP was added to each mixture to adjust the weight percent of PAA in each mixture to 8 wt%. The mixed solutions were stirred vigorously at room temperature for one day. To fabricate the SiO_2-polyimide nanocomposite films, the SiO_2-PAA nanocomposite dispersions were poured into glass dishes and degassed in vacuum.Then, the SiO_2-PAA nanocompsite dispersions were heated at 60 °C for 12 h, 100 °C for 1 h, 150 °C for 1 h, 200 °C for 1 h, 250 °C for 1 h, and finally at 350 °C for 1 h 30 min in a vacuum oven to carry out the imidization process as suggested in the literature.[26] The SiO_2-polyimide nanocomposite films were obtained by peeling them off from the glass substrates.

Characterization

To study the surfaces of the silica nanoparticles, Fourier-transform infrared (FT-IR) spectra were recorded using a NICOLET iS10 system. Hydrodynamic size of SiO_2 in EtOH, DETAS-SiO_2 in EtOH, and P-SiO_2 in NMP was measured five times and averaged at room temperature using the dynamic light scattering (DLS, Zetasizer, Malvern instruments). The zeta potential values of the particles in ethanol were measured using a zetameter (Zetasizer, Malvern instruments). ^{13}C Cross polarization/magic angle spinning (CP/MAS) nuclear magnetic resonance (NMR) spectra were measured using a Bruker Avance 400MHz WB. Transmission electron microscopy (TEM) images were acquired using a Hitachi-7600 instrument operated at 100 kV. Nanocomposite films were microtomed (thickness: ~100 nm) in a model MT-X Ultramicrotome with CR-X, Boeckeler Instruments, Inc.

Thermal gravimetric analysis (TGA) measurements were performed using an SDT Q600 apparatus (TA Instruments Inc.). TGA was performed by pre-heating the sample at 100 °C for 60 min and then heating it from 100 °C to 1000 °C at a heating rate of 10 °C/min under N_2-atmosphere. Transmittance was measured using a UV-Vis spectrometer (Sinco, S-3100). Thermal mechanical analyses (TMA), using a TMA-Q400 system, were performed to measure the T_g and CTE of the nanocomposite films under the tension mode (load = 50 mN), by heating them from 25 °C to 400 °C at a heating rate of 5 °C/min under nitrogen.

Nanoindentation tests were performed on 50–60 μm-thick polyimide and SiO_2-PI nanocomposite films using an Ultra Nanoindentation Tester (UNHT, CSM instruments). The loading and unloading rates were both 250 mN/min. A holding time of 3 s was maintained at the maximum load. At least seven indentations were performed on each sample, and the average values were determined.

In an indentation test, hardness is defined as the indentation at the maximum load, P_{max}, divided by the projected area of tip-sample contact, A, and is calculated for a perfect Berkovich indenter as follows:

$$H = \frac{P_{max}}{A}$$

$$A = 24.5 h_c^{\,2}$$

Here the contact depth, h_c, can be determined by taking into account the response of the material's elastic deflection, h_d:

$$h_c = h_{max} - h_d$$

$$h_c = \varepsilon \frac{P_{max}}{S}$$

where h_{max} and S are the maximum indentation depth and initial unloading stiffness, respectively, and ε is a geometrical constant (0.75 for a Berkovich indenter). The contact stiffness of the sample, S, is given by the initial unloading slope.

The effective elastic modulus is formulated in terms of the unloading slope S and contact area A as

$$E_{eff} = \frac{\sqrt{\pi} \cdot S}{2 \cdot \beta \cdot \sqrt{A}}$$

For a Berkovich indenter, the indenter geometry parameter β is 1.034.

Results and discussion

Fig. 2a shows a TEM image of silica nanoparticles with diameters of 30±4 nm. And hydrodynamic size of SiO_2 measured by DLS was 46±1 nm (Fig. S1a), which indicated that SiO_2 were well dispersed in ethanol without any aggregation. As shown in the Fig. S2, unmodified SiO_2 nanoparticles tend to generate the large aggregation within the polyimide matrix. Therefore, surface modification is needed to improve dispersion stability of SiO_2 in polyimide matrix. To introduce a ligand with a structure similar to the repeating units of polymer on the silica surface, a large number of amine groups were introduced on the silica surface by attaching DETAS to the surface of the SiO_2 nanoparticles to generate DETAS-SiO_2, and then, the amine groups of DETAS-SiO_2 were reacted with phthalic anhydride in EtOH (Fig. 1a), to form

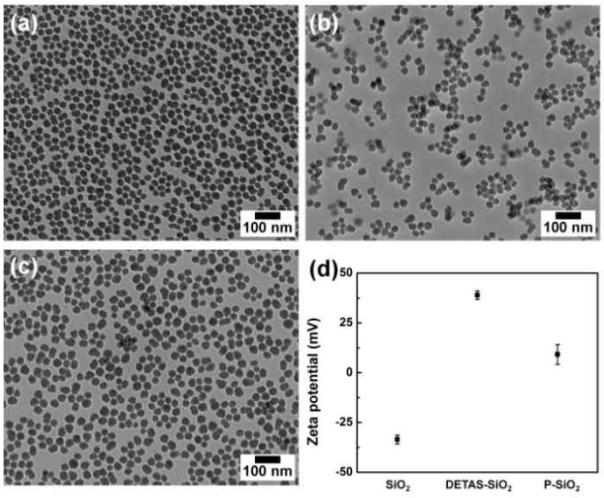

Fig. 2 TEM images of (a) as-prepared silica nanoparticles, (b) DETAS-SiO_2, and (c) P-SiO_2. (d) zeta potential values of as-prepared and modified silica nanoparticles in EtOH.

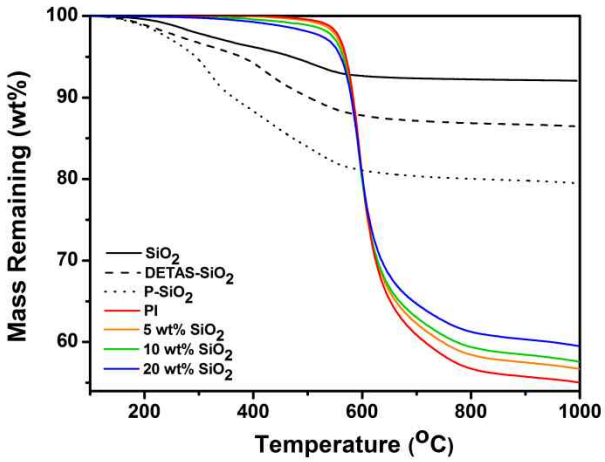

Fig. 3 TGA curves for bare silica, modified silica nanoparticles (DETAS-SiO_2 and P-SiO_2), neat polyimide film, and SiO_2- polyimide nanocomposite films with various SiO_2 contents.

imide or amic acid groups *via* the phthalic anhydride-ring opening reactions. As was expected, the amic acid moiety on the nanoparticle surfaces acted as a plasticizer by interacting with the polymer chains as reported that dimethyl phthalate could be used as plasticizers for polyimide to decrease T_g and T_d.[27]

After the modification, the surfaces of the SiO_2 nanoparticles was characterized by FT-IR, solid-state ^{13}C-NMR, zeta-potentail, and TGA. A strong absorption band at 1710 cm^{-1}, which corresponded to a C=O stretching vibration from the amic acid moiety, was clearly observed in the FT-IR spectrum of the P-SiO_2 (see the Supporting Information Fig. S3). In addition, new peaks at 110–130 ppm and 160–170 ppm, corresponding to aromatic carbons and carbonyl carbon, respectively, were found in the solid-state ^{13}C-NMR spectrum of the P-SiO_2 (see the Supporting Information Fig. S4). As

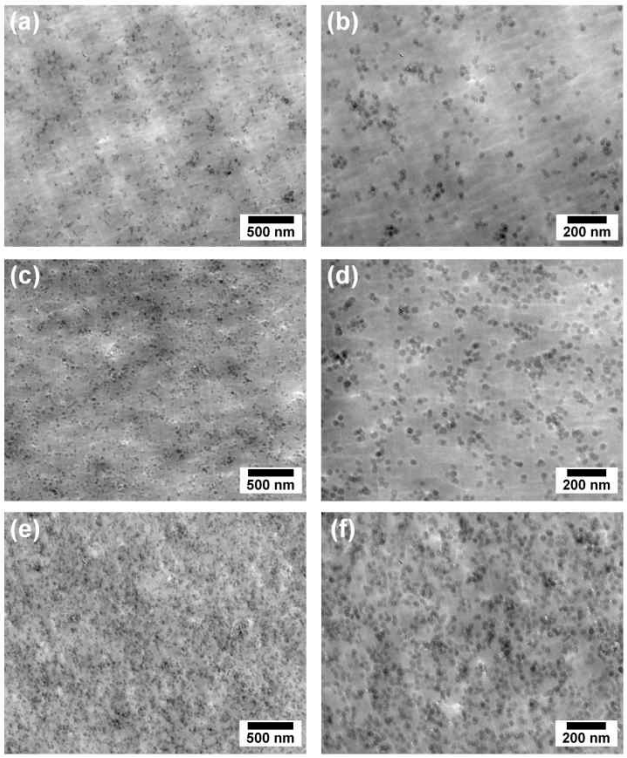

Fig. 4 Cross-sectional TEM images of SiO_2-PI nanocomposite films: (a, b) 5, (c, d) 10, and (e, f) 20 wt% of SiO_2. (a), (c) and (e) are under low magnification; (b), (d) and (f) are under high magnification.

shown in Fig. 2a–c, the nanoparticles were well dispersed in the solvents (EtOH and NMP) without showing any significant changes in size or shape during the surface modification reactions. Furthermore, the surface charge of the bare SiO_2 generated a negative zeta potential of -33.6 mV due to a hydroxyl group, as shown in Fig. 2d. After attaching DETAS, however, the zeta potential changed from -33.6 mV to 38.9 mV, which is attributed to positively charged amine groups in the DETAS on the silica surface, even neutral conditions. The zeta-potential of the P-SiO_2 was 9.1 mV since most of the amine groups of the DETAS formed neutral imide linkages with phtalic anhydride and some amic acid units had Zwitter-ion-type charges.

TGA curves for bare SiO_2, DETAS-SiO_2, and P-SiO_2 are shown in Fig. 3. The amount of weight loss gradually increased in the temperature range from 100 to 1000 °C. An additional 5.6 % and 12.6 % weight loss resulted from the attached organic units on the surfaces of the SiO_2 nanoparticles after the surface modification. The mole percentage of organic groups on the surface of SiO_2 nanoparticles could be calculated from TGA data as summarized in Table S1.

Since polyamic acid was dissolved in and is usually processed in NMP, the P-SiO_2 was dispersed in the NMP in order to homogeneously incorporate the SiO_2 nanoparticles in the poly-amic acid. As shown in Fig. 2c and Fig. S1c, the P-SiO_2 nanoparticles were well dispersed in NMP without generating aggregation. Furthermore, the dispersed P-SiO_2 solution in

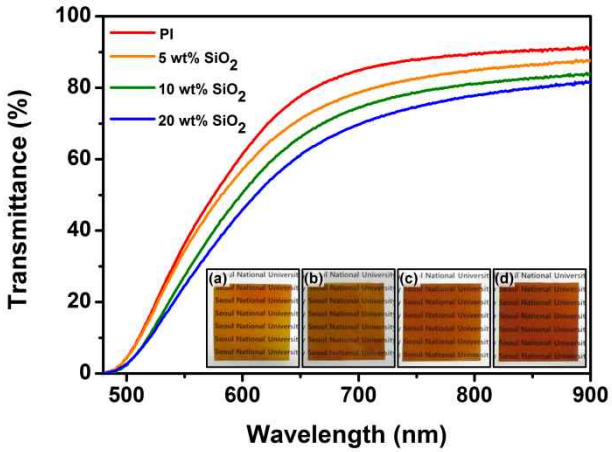

Fig. 5 Transmittance spectra of neat PI film and SiO_2-PI nanocomposite films with various SiO_2 contents. Inset: digital photographs of nanocomposite films clearly showing the transparency; (a) neat PI film, SiO_2-PI nanocomposite films with (b) 5, (c) 10, and (d) 20 wt% of SiO_2.

NMP showed the excellent long-term stability over the one year (Fig. S1d). Four different SiO_2-polyamic acid nanocomposite solutions (5, 10, 20, and 40 wt% of SiO_2) were prepared by mixing the appropriate amounts of polyamic acid solution with the P-SiO_2 nanoparticles dispersed in the NMP solution. The SiO_2-polyimide nanocomposite films were produced using the thermal imidization method, by gradually heating the SiO_2-polyamic acid nanocomposite solution up to 350 °C, as described in the experimental section. Fig. 4 shows cross-sectional TEM images of SiO_2-PI nanocomposite films. It was clearly observed that the silica nanoparticles were homogeneously dispered in the polyimide matrices without showing signs of aggregation. This indicates that the ligands on the SiO_2 surface have similar chemical structures to the repeating units of the polyimide, and thus, the compatibility between the polymer chain and the nanoparticles is enhanced. As a result, aggregations were not observed in any of the SiO_2-polyimide nanocomposite films having up to 40 wt% of SiO_2 nanoparticles (Fig. S5). However, SiO_2-polyimide nanocomposites films became brittle beyond 40 wt% of the incorporated SiO_2 nanoparticles. Therefore, further measurements were performed with SiO_2-PI nanocomposites having the content of SiO_2 nanoparticles under 20 wt%.

Transparency of SiO_2-PI nanocomposite films, which can be measured using a UV-Vis spectrometer, is another important property for optical applicaions. Strong absorption in the UV-Vis region from all of the samples is attributed to an intrinsic feature of polyimides (Fig. 5), which exhibit charge transfer interactions between electron donor and acceptor[10] even though the thickness of the PI films ranged from 50 μm to 60 μm. Although the transparency gradually decreased with increasing silica content, no serious degradation in transparency was found in any of the samples. This result also indicates that the silica nanoparticles are homogeneously dispersed in the polyimide matrices; thus, scattering of light in the visible region is negligible.

T_g values of the PI and SiO_2-PI nanocomposite films were determined by TMA, and the results are listed in Table 1; the T_g values of the nanocomposites gradually declined as the silica content increased. Because of the large surface area of the nanoparticles, the interface between the polymer and the nanoparticle can change and affect the thermal properties of the nanocomposites.[28] We assume that ligands on the nanoparticle surfaces acted as plasticizers for the polyimide. As a result, the chain kinetics of the polymer are changed at the polyimide-nanoparticle interface regions,[29] and thus, T_g decreases from 381.3 to 363.3 °C as the SiO_2 content increases. This result indicates that SiO_2-polyimide nanocomposites have better processability due to the plasticizing effect of the P-SiO_2 surface ligands.

TGA curves for the SiO_2-PI nanocomposite films with various silica contents are also shown in Fig. 3. For all of the samples, almost no weight loss was found up to around 300 °C, and then, the films gradually decomposed at higher temperatures. The T_d values of the nanocomposites, which were determined as the temperatures at which 5 % weight loss occured on the TGA curves, are summarized in Table 1. Although the T_d values decreased slightly with inceasing silica content, T_d for each of the nanocomposites was higher than 500 °C, indicating good thermal stability for practical applications. The decreasing T_d values with increasing silica content can be explained by the same reasoning as for the decreasing of T_g values. As expected, the remaining weight (wt%) at 1000 °C was proportional to the amount of silica nanoparticles in each of the polyimide films.

To quantify the effect of the SiO_2 nanoparticles on the thermal expansion of the PI nanocomposites, TMAs were performed. Fig. S6 shows the thermal expansion curves for the PI and nanocomposite films in the temperature range from 100

Table 1. Thermal and mechanical properties of PI and SiO_2-PI nanocomposite films

	T_d (°C)[a]	T_g (°C)[b]	CTE (10^{-6}/°C)[c]	Hardness (MPa)	Modulus (GPa)
Polyimide	570.1	381.3	33.9	215.4±2.5	3.20±0.03
5 wt% SiO_2-PI	567.7	379.1	30.8	229.7±1.6	3.48±0.04
10 wt% SiO_2-PI	564.7	376.3	30.6	249.9±2.8	3.50±0.05
20 wt% SiO_2-PI	560.3	363.3	27.8	283.9±4.3	3.71±0.05

[a] Temperature at which 5 % weight loss was recorded by TGA; [b] T_g determined by TMA; [c] CTE was determined over a range of 100–250 °C.

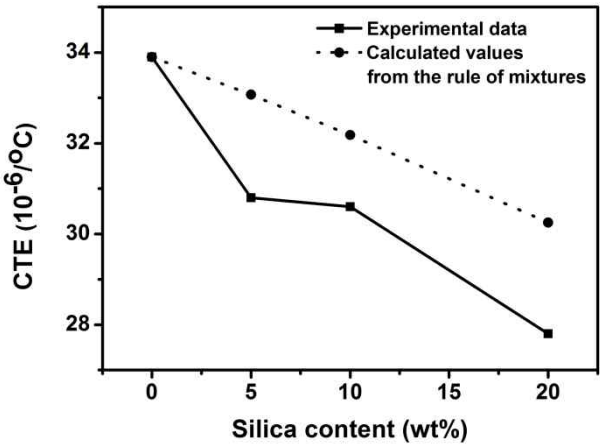

Fig. 6 CTE values for neat PI and SiO_2-PI nanocomposite films

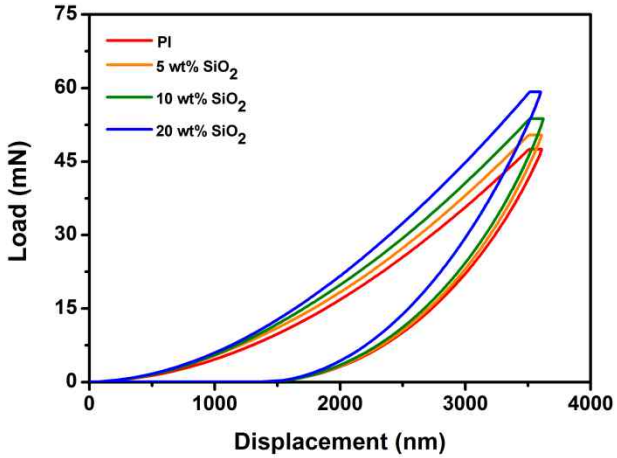

Fig. 7 Load *vs.* indenter displacement for neat PI film and SiO_2-PI nanocomposite films with different SiO_2 contents

to 250 °C. The coefficient of thermal expansions, α, for the nanocomposite films, which were calculated based on the thermal expansion curves by following equation, are shown in Table 1.

$$\alpha = \frac{1}{L_0}\frac{\Delta L}{\Delta T}$$

Where L_0 is the initial length of sample and ΔL is the length change at a given temperature difference (ΔT). As expected, reductions in the CTE are observed with the incorporation of silica nanoparticles into the PI matrix. The CTEs for neat PI and nanocomposites with 5, 10, and 20 wt% SiO_2 were 33.9, 30.8, 30.6 and 27.8 °C $^{-1}$, repectively, as shown in Fig. 6 SiO_2 has a relatively low CTE (~0.55×10^{-6} °C $^{-1}$) in comparison with PI (33.9×10^{-6} °C $^{-1}$), resulting in reductions of the thermal expansion of the nanocomposites as the SiO_2 content increases. In order to predict the theoretical CTE values of the nanocomposites, the CTE of each nanocomposite was calculated by the simplest rule of mixtures model,[30] assuming that there is no interfacial interaction between the polymer and the nanoparticles (see the Supporting Information for the detailed calculation and Table S2). These calculated values are shown along with the experimental data in Fig. 6; significant differences between the two sets of data are apparent confirming the important interfacial interaction between the, polymer and the surface-modified SiO_2 nanoparticles.

Nanoindentation tests were performed to investigate the effect of nanoparticle reinforcement on the nanocomposite's mechanical properties. Fig. 7 shows load-displacement curves for neat PI and the nanocomposites with various silica contents. The similarities among the curves indicates that the nanocomposites are based on polyimide matrices. The curves gradually shift upwards and the maximum penetration depth decreases as the silica content in the PI matrices increases, since silica nanoparticles lead to nanocomposites with high resistance to plastic deformation.[31, 32] The elastic displacement is recovered during unloading. The initial unloading slopes (stiffness, *S*) increase with silica content, and thus, the effective

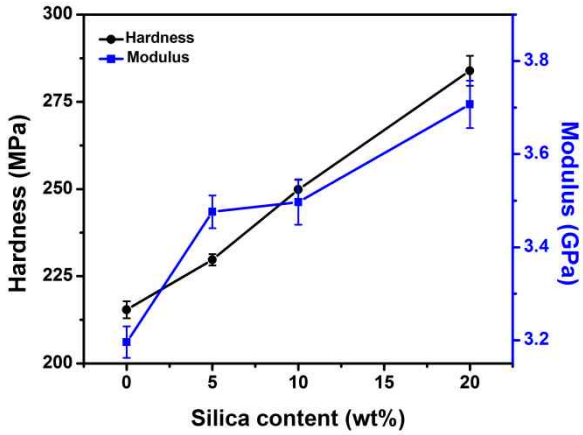

Fig. 8 Hardness and effective elastic modulus values for neat PI and SiO_2-PI nanocomposite films with different SiO_2 contents.

elastic moduli are enhanced. The average hardness *H* and effective elastic modulus E_{eff} values are calculated from the nanoindentation curves using the Oliver-Pharr method[33] and are shown in Fig. 8. Both *H* and E_{eff} for the polyimide nanocomposites increased markedly with the SiO_2 content in the polyimide. This result indicated that the SiO_2 in the polymer matrix acts as a reinforcement against deformation, thus improving it's mechanical properties.

Conclusions

We successfully prepared SiO_2-polyimide nanocomposites by attaching a DETAS to SiO_2 surfaces and subsequently reacting them with phthalic anhydride in order to increase the compatibility and generate interfacial interactions between the silica nanoparticles and the polyimide. The modified silica nanoparticles were homogeneously dispersed in polyimide matrices up to 20 wt% of SiO_2 nanoparticles, without showing any microphase aggregation or significant decreases in transparency for any of the nanocomposite films. T_d and T_g values decreased with increasing silica content, probably due to the plasticizing effect of the surface ligands on the P-SiO_2. CTE values decreased with increases in the silica content; the CTE

value of 20 wt% SiO_2-PI nanocomposite was 27.8×10^{-6} $°C^{-1}$, which is significantly smaller than that of parent polyimide (33.9×10^{-6} $°C^{-1}$). The nanoindentation results showed that both H and E_{eff} were enhanced with increasing silica content, corroborating the potential of these modified SiO_2 nanofillers for applications requiring a low CTE and high thermal stability, along with optical transparency.

Acknowledgements

This research was supported by the Pioneer Research Center Program through the National Research Foundation of Korea funded by the Ministry of Science, ICT and Future Planning (2012-0009552). This research was also supported by the Converging Research Center Program through the Ministry of Science, ICT and Future Planning, Korea (2013K000206). Y.-J. Kim is grateful for the award of a BK21 fellowship. The authors thank J. H. Kim and Prof. B.-H. Sohn for helping with the preparation of cross-sectional TEM samples by microtoming.

Notes and references

[a] Department of Chemistry, Seoul National University, Seoul 151-747, Korea. E-mail: jinklee@snu.ac.kr; Fax: +82-2-882-1080; Tel: +82-2-879-2923
[b] Department of Materials Science and Engineering, Seoul National University, Seoul 151-744, Korea
[c] Present address: Department of Medicine, Emory University, Atlanta, GA 30322, USA

† Electronic supplementary information (ESI) available: FT-IR, solid ^{13}C CP/MAS NMR spectra, and DLS data of SiO_2, DETAS-SiO_2, and $PSiO_2$, TEM images of SiO2-PI composites, thermal expansion of PI and composite films, calculation details of CTE.. See DOI: DOI: 10.1039/x0xx00000x

1. C. L. Lu and B. Yang, *J. Mater. Chem.*, 2009, **19**, 2884.
2. R. P. Ortiz, A. Facchetti and T. J. Marks, *Chem. Rev.*, 2010, **110**, 205.
3. W. E. Jones, J. Chiguma, E. Johnson, A. Pachamuthu and D. Santos, *Materials*, 2010, **3**, 1478.
4. H. Zou, S. S. Wu and J. Shen, *Chem. Rev.*, 2008, **108**, 3893.
5. G. Schottner, *Chem. Mater.*, 2001, **13**, 3422.
6. J. Y. Wang, W. Chen, A. H. Liu, G. Lu, G. Zhang, J. H. Zhang and B. Yang, *J. Am. Chem. Soc.*, 2002, **124**, 13358.
7. R. Barbey, L. Lavanant, D. Paripovic, N. Schuwer, C. Sugnaux, S. Tugulu and H. A. Klok, *Chem. Rev.*, 2009, **109**, 5437.
8. S. Ghosh, S. K. Goswami and L. J. Mathias, *J. Mater. Chem. A*, 2013, **1**, 6073.
9. Y. Li, S. Y. Fu, Y. Q. Li, Q. Y. Pan, G. S. Xu and C. Y. Yuu, *Compos. Sci. Technol.*, 2007, **67**, 2408.
10. T. Hasegawa and K. Horie, *Prog. Polym. Sci.*, 2001, **26**, 259.
11. S. H. Hsiao, W. J. Guo, C. L. Chung and W. T. Chen, *Eur. Polym. J.*, 2010, **46**, 1878.
12. B.-K. Chen, T.-Y. Wu, C.-H. Lin and J.-M. Wong, *Fibers. Polym.*, 2013, **14**, 1051.
13. Z. D. Wang, J. J. Lu, Y. Li, S. Y. Fu, S. Q. Jiang and X. X. Zhao, *Compos. Part A-Appl. S.*, 2006, **37**, 74.
14. D. V. Zhmurkin, T. S. Gross, L. P. Buchwalter and F. B. Kaufman, *J. Electron. Mater*, 1996, **25**, 976.
15. J. C. Tang, G. L. Lin, H. C. Yang, G. J. Jiang and Y. W. Chen-Yang, *J. Appl. Polym. Sci.*, 2007, **104**, 4096.
16. S. Y. Fu and B. Zheng, *Chem. Mater.*, 2008, **20**, 1090.
17. S. H. Hsiao, G. S. Liou and L. M. Chang, *J. Appl. Polym. Sci.*, 2001, **80**, 2067.
18. D. Knopp, D. P. Tang and R. Niessner, *Anal. Chim. Acta.*, 2009, **647**, 14.
19. Z. Ahmad and J. E. Mark, *Chem. Mater.*, 2001, **13**, 3320.
20. G. Ragosta and P. Musto, *Express Polym. Lett.*, 2009, **3**, 413.
21. B. K. Chen, T. M. Chiu and S. Y. Tsay, *J. Appl. Polym. Sci.*, 2004, **94**, 382.
22. Z. P. Shang, C. L. Lu, X. D. Lu and L. X. Gao, *J. Appl. Polym. Sci.*, 2008, **109**, 3477.
23. J. C. Tang, H. C. Yang, S. Y. Chen and Y. W. Chen-Yang, *Polym. Composite*, 2007, **28**, 575.
24. W. Stober, A. Fink and E. Bohn, *J. Colloid. Interf. Sci.*, 1968, **26**, 62.
25. H. S. Jung, D. S. Moon and J. K. Lee, *J. Nanomater.*, 2012, **2012**, 593471.
26. H. Li, G. Liu, B. Liu, W. Chen and S. Chen, *Mater. Lett.*, 2007, **61**, 1507.
27. E. Totu, E. Segal and A. K. Covington, *J. Therm. Anal. Calorim.*, 1998, **52**, 383.
28. Y. Y. Sun, Z. Q. Zhang, K. S. Moon and C. P. Wong, *J. Polym. Sci. Pol. Phys.*, 2004, **42**, 3849.
29. B. J. Ash, L. S. Schadler and R. W. Siegel, *Mater. Lett.*, 2002, **55**, 83.
30. H. S. Katz and J. V. Mileski, *Handbook Of Fillers For Plastics*, Springer, 1987, 49.
31. H. N. Dhakal, Z. Y. Zhang and M. O. W. Richardson, *Polym. Test.*, 2006, **25**, 846.
32. Y. C. Hu, L. Shen, H. Yang, M. Wang, T. X. Liu, T. Liang and J. Zhang, *Polym. Test.*, 2006, **25**, 492.
33. W. C. Oliver and G. M. Pharr, *J. Mater. Res.*, 1992, **7**, 1564.

Polyimide nanocomposites with functionalized SiO_2 nanoparticles: Enhanced processability, thermal and mechanical properties

Young-Jae Kim,[a] Jong-Heon Kim,[b] Shin-Woo Ha,[a,c] Dongil Kwon,[*b] Jin-Kyu Lee[*a]

[a]Department of Chemistry, Seoul National University, Seoul 151-747, Korea

[b]Department of Materials Science and Engineering, Seoul National University, Seoul 151-744, Korea

[c]Present address: Department of Medicine, Emory University, Atlanta, GA 30322, USA

Highlight (20-30 words)

SiO_2-polyimide nanocomposites having enhanced processability, thermal and mechanical properties were easily fabricated by the surface modification of silica nanoparticles with functional groups having chemical and structural similarity to polyimide chain.

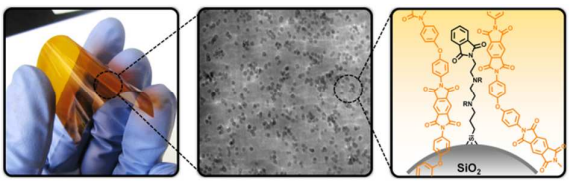

Table of contens